Atomic relaxation in silicon carbide polytypes

1990 J. Phys.: Condens. Matter 2 5115

(http://iopscience.iop.org/0953-8984/2/23/003)

J. Phys.: Condens. Matter 2 (1990) 5115–5134. Printed in the UK

Atomic relaxation in silicon carbide polytypes

C Cheng, Volker Heine and R J Needs
TCM Group, Cavendish Laboratory, Madingley Road, Cambridge CB3 0HE, UK

Received 29 December 1989

Abstract. The relaxed structures of the ⟨1⟩, ⟨2⟩, ⟨23⟩ and ⟨3⟩ polytypes of silicon carbide are calculated using the pseudopotential total-energy technique with norm-conserving pseudopotentials and the local density approximation to the exchange–correlation energy. A 'tension model' is proposed to account for the atomic forces and stresses of the ideal structures and the results of the detailed relaxed structures. We also deduce the force field due to an isolated antiphase boundary from the calculated atomic forces of the ideal structures. The energies associated with these relaxations are about 1 meV per SiC pair of atoms per antiphase boundary. In order to calculate it, we have developed a new formulation, which should be of wider use in calculating relaxation energies. We discuss the different effects of longitudinal and transverse relaxations on the stability of the polytypes, particularly ⟨23⟩ as a possible intermediate phase between ⟨2⟩ and ⟨3⟩.

1. Introduction

Silicon carbide (SiC) forms in dozens of polytypes [1], each of which is a different periodic stacking sequence of identical SiC layers. The phenomenon of polytypism in SiC has been studied for many years, and the present work is one of a series of papers discussing both static and phonon effects [2–4]. A number of different theories have been proposed at various times involving both equilibrium and non-equilibrium effects [1, 5]. In our previous work [2] we calculated the energies of several SiC polytypes and found that the experimentally observed polytypes are in general lower in energy than those that are not observed. These results imply that the observed polytypes are equilibrium, phases at the high temperatures of growth with the structures becoming frozen-in on cooling. We also calculated in a companion paper [4] (to be referred to as I) the phonon contribution to the free energy and found that it stabilised the polytype ⟨23⟩ (in Zhdanov notation [6], see below) as an intermediate phase between the structures ⟨2⟩ and ⟨3⟩.

Although the polytypes of SiC consist of different stackings of the same basic unit, small relaxations of the positions of the atoms can occur because of the different symmetries of the structures. In this paper we study the detailed structure of four SiC polytypes, including the most commonly observed ones, using *ab initio* total-energy calculations and relaxing the atomic positions and lattice parameters to minimise the energy. These relaxations were neglected in the previous calculations in [2]. The purpose is twofold. (i) The pattern of the relaxations in bond lengths and bond angles is at first sight rather surprising and of interest in its own right. We find that from all our calculations that the percentage deviations of the bond angles from the ideal tetrahedral

0953-8984/90/235115 + 20 $03.50

value are smaller than the percentage differences in bond lengths. This is the opposite of what one finds in, say, amorphous silicon, and runs counter to the fact that force constants for bond bending are weaker than for bond stretching. The detailed results and discussions are presented in section 4. (ii) The most important point is that the relaxation energies can contribute to stabilising polytype structures. We shall discuss this generally and include results for the polytype ⟨23⟩ specifically. We refer to paper I for a wider discussion of polytype stability, temperature effects, etc., into which the results of the present work are to be inserted. The short answer is that the relaxation contributions to polytype stability/instability (there are effects of both signs) seem to be smaller than the effect of the phonon free energy.

Let us outline the conceptual framework for the present investigation. The structures of SiC polytypes consist of different stackings of layers in what would be the (111) direction of the cubic zincblende structure. Each layer can be placed on top of the one below in two different orientations. The two possibilities are denoted by an up spin '+' and a down spin '−'. In the Zhdanov notation [6] the structure is written in terms of the widths of bands of parallel spins. For instance, the cubic structure is ⟨∞⟩, wurtzite is ⟨1⟩ and the three most commonly observed polytypes in order of prevalence, 6H, 4H and 15R, are written as ⟨3⟩, ⟨2⟩ and ⟨23⟩, respectively. We shall use the Zhadanov notation throughout the rest of this paper.

In our calculations, we start with the 'ideal' structures of ⟨1⟩, ⟨2⟩, ⟨3⟩ and ⟨23⟩ in which all bond angles have the perfect tetrahedral value and all bond lengths are equal to one another and equal to that in the cubic phase ⟨∞⟩. We do total-energy calculations with norm-conserving pseudopotentials in density-functional theory with the local density approximation for exchange and correlation as reported previously [2]. From the self-consistent wavefunctions we now evaluate the stresses σ_{zz} and $\sigma_{xx} = \sigma_{yy}$, as well as the Hellmann–Feynman forces f_i on the atoms (which are all in the z direction, i.e. the stacking direction). We then relax the atomic positions and lattice constants a and c such that the forces and stresses are zero: to be precise, we relax the stresses to equal that of the cubic structure, which was isotropic but not exactly zero (section 2). In this way the relaxation energies are obtained. The relaxation energy is defined as the energy difference between a polytype in the ideal structure at the volume that is the volume of the cubic phase at zero stress and the relaxed polytype at zero stress (section 2). In order to understand the relaxations, it is in some ways easier to discuss the forces and stresses in the ideal structures than the relaxations themselves, because in the ideal structures one does not have the complicated interplay between the relaxation of one plane and another, nor between atomic relaxation and change of lattice constants. Decomposing forces into the ion–ion and electron–ion contributions for Si and C atoms allows us to build up a clear picture of what is the effect of a boundary on an atom and how far the effect extends (section 3). In order to clarify the picture even further, a very simple 'tension model' is proposed. In this model, the interatomic bonds are represented by springs whose tensions give the forces and stresses of the ideal structure and hence relate these to each other. The bond angle forces are not included. The tensions interpret some of the results of the relaxed structures. The computed longitudinal relaxations of the spacings between atomic layers are qualitatively consistent with the tensions suggested by the model.

The second aim (ii) of this paper is to investigate whether relaxations could stabilise long-period polytypes such as are observed for SiC. Previous pseudopotential total-energy calculations [2] of ideal structures have shown that the energies of ⟨2⟩ and ⟨3⟩ are nearly identical. Phonon calculations in paper I showed ⟨2⟩ has lower free energy than

$\langle 3 \rangle$ at low temperature, but $\langle 3 \rangle$ becomes stable above $T = T_0$ where these two have the same free energy. The question is whether the simplest intermediate phase $\langle 23 \rangle$ is a stable phase. To a good approximation the polytype $\langle 23 \rangle$ is just an alternation of 2-bands and 3-bands taken from the simple polytypes $\langle 2 \rangle$ and $\langle 3 \rangle$, so that we write for the energy (per SiC pair of atoms)

$$E_{\langle 23 \rangle} = [(2/5)E_{\langle 2 \rangle} + (3/5)E_{\langle 3 \rangle}] + \Delta \tag{1.1}$$

where Δ is a correction to the simple approximation in square brackets. Clearly a negative value of Δ would stabilise $\langle 23 \rangle$ as an intermediate phase between $\langle 2 \rangle$ and $\langle 3 \rangle$ in a phase diagram. The calculations in paper I show that the phonon contribution to Δ is negative. We shall study the relaxation contribution Δ_r to Δ in the present paper. Note that we are calculating only the energies at temperature $T = 0$, the relaxation energies being separate from and in addition to the phonon free energies of I.

A slightly different view is to treat an arbitrary polytype as bands of cubic stacking separated by antiphase boundaries (hereafter 'boundaries' for short). The energy is then written as

$$E = E_{\langle \infty \rangle} + \beta x + \sum c_m I_m \tag{1.2}$$

where β is the chemical potential for introducing a boundary into the cubic material of energy $E_{\langle \infty \rangle}$ and x is the concentration of boundaries per SiC double atomic layer, i.e. the inverse mean band width. The I_m are boundary–boundary interactions (BBI) with coefficients c_m depending on the polytype. For instance, we have

$$E_{\langle 2 \rangle} = E_{\langle \infty \rangle} + (1/2)\beta + (1/2)I_2 + (1/2)I_4 + \ldots . \tag{1.3}$$

In general, it is necessary to distinguish between nearest-neighbour (NN), next nearest-neighbour (NNN), etc., BBI as discussed in I. However, the analysis of forces (section 3) shows that for the relaxation energy $I_m^{\mathrm{NN}} \simeq I_m^{\mathrm{NNN}}$. It is easy to see that Δ in (1.1) can be expressed to leading terms as

$$\Delta \simeq -(1/5)(I_4^{\mathrm{NNN}} + I_6^{\mathrm{NNN}} - 2I_5^{\mathrm{NNN}}). \tag{1.4}$$

The stabilisation of phase $\langle 23 \rangle$ therefore requires at least next nearest-neighbour BBI.

The relaxation energy of a polytype can be interpreted in terms of a BBI due to the overlap of the force fields of neighbouring boundaries. If we consider an isolated boundary in the cubic structure, it will produce locally a pattern of forces f_i and stresses falling off with distance in some way. When there are two boundaries, their force fields will overlap and produce a BBI when the structure is relaxed. The sign and order of magnitude of the BBI is discussed in section 3. Comparison and analysis of the calculated forces for $\langle 2 \rangle$, $\langle 3 \rangle$ and $\langle 23 \rangle$ show that the force fields clearly overlap sufficiently to give nearest-neighbour BBI but extend only a tiny bit to the next nearest-neighbour boundary. The contribution to Δ is thus, in accordance with (1.4), quite small. We are at the very limit of what can be calculated but the Δ_r from relaxations appears to be somewhat smaller than the phonon free-energy contribution in paper I. The relaxation of the lattice parameters calls for special comment. Part of the total relaxation energy arises from the transverse relaxation of the a lattice parameter. Pictorially, we can say that the 2-bands as seen in the pure phase $\langle 2 \rangle$ 'want' to have a certain a lattice parameter and the 3-bands 'want' to have a slightly larger one, as shown by the phase $\langle 3 \rangle$. In the polytype $\langle 23 \rangle$ or higher polytypes, the 2-bands and 3-bands therefore have to expand and shrink laterally a little in order to fit together. This effect always leads to an attractive BBI, as has been discussed for other materials [7], i.e. it makes polytypes unstable with respect to the

constituent phases ⟨2⟩ and ⟨3⟩. However, we estimate its contribution to Δ to be about 1.5×10^{-6} eV per SiC pair, smaller than the phonon free energies in paper I. Although it is part of the total relaxation energy, we can split it off, because it is manifested purely in the transverse stress $\sigma_{xx} = \sigma_{yy}$ of the ideal structure, is of a long-range nature that we can think of in terms of macroscopic continuum theory, is of constant sign and would give zero forces f_i in the ideal structure if present alone. It is discussed in section 5. The situation is rather different regarding the longitudinal relaxation of the c lattice parameter. Again we can envisage stacking 2-bands and 3-bands, each with its own thickness as in pure ⟨2⟩ and ⟨3⟩ differing slightly from one another. But the c lattice parameter does not involve any constraint or matching of the two types of band: we expect the total thickness in the z direction to be additive, without any long-range effect analogous to that of the transverse relaxation above. Of course, there will in general be a local expansion (or contraction) of the atomic layer spacings in the z direction around the boundaries in order to relax the average σ_{zz} stress. But this is part of the local effect around each boundary. Certainly the two are inherently combined in our tension model. We discuss this in detail in section 5 because it had earlier been suggested by Bruinsma and Zangwill [8] from an appealingly simple but rather general model that longitudinal relaxation would more or less automatically always stabilise an infinite sequence of polytypes. Such a conclusion would clearly be of great interest and relevance, but it seems to us that their model is not really appropriate to describe the physics, a point they now acknowledge [9].

Finally we include in this paper (section 6) a short item needed for completeness in our wider treatment of SiC polytypes, although not directly related to relaxations. Are there effects in the electronic structure of the *ideal* structures that contribute to I_m? The previous total-energy calculations showed significant values of I_1 and I_2. Those calculations were analysed in terms of interplanar interactions J_n, etc., and the BBI I_m is expressible in terms of the J_n, etc., with $n = m + 1, m + 2, \ldots$, as discussed in paper I. Unfortunately J_3 and therefore I_2 were as far as the explicit calculations could go, but in section 6 we make estimates for larger separations. The conclusion is that we think they are even smaller than the rather smaller free-energy contributions calculated in paper I. The connection with the present work is as follows. If we introduce an isolated boundary into what is otherwise cubic material, the boundary causes a local perturbation of the electronic structure. One manifestation is the force field f_i mentioned above, another is the contribution J_n to reversing the orientation of a layer that is n layers away. A similar effect is the force field due to displacing a simple atom as in the analysis of the phonon spectrum in I. All are the result of a local perturbation of the electronic structure and hence all may be expected to have a similar range. Thus we can make an order-of-magnitude estimate of the more distant J_n from what is known of the f_i (section 3) and of the phonon force constants [4].

2. Calculating the atomic relaxations

The relaxed atomic coordinates and the associated relaxation energies of the different polytypes were calculated by minimising the total energy of the system with respect to both changes in the size and shape of the unit cell as well as changes in the atomic positions within the unit cell. For the energy calculations we used the same pseudopotential total-energy techniques as in our earlier work on SiC polytypes [2]. For a review of this calculational method and applications of it, we refer the reader to the recent review

article by Ihm [10]. In order to calculate atomic relaxations, it is advantageous to calculate not only the energy as a function of the atomic positions but also the forces on the atoms and the stress on the unit cell. Knowledge of the forces and stress make it much easier to locate the energy minimum because they give the direction of change in parameter space that lowers the total energy. In our work the forces are calculated from the Hellmann–Feynman theorem [11] and the stress tensor is obtained using a generalisation of the virial theorem [12].

In our calculations we have used the pseudopotentials calculated by Bachelet *et al* [13], who used the method of generation due to Hamann *et al* [14]. Previous calculations [15] using these pseudopotentials gave the lattice constant of the zincblende $\langle\infty\rangle$ phase of SiC to within 1% of the experimental value. Usually the lattice constants calculated using the local density approximation are a little smaller than the experimental values. Such calculations are performed by calculating the total energy as a function of volume and locating the volume at which the energy is a minimum. As the volume is increased, the number of waves in the basis set is increased so as to keep the basis set energy cut-off fixed. The results of many calculations have shown that this procedure results in accurate values of the equilibrium volume, so that the error due to the basis set truncation is small. On the other hand, calculations of the stress tensor using the generalised virial theorem correspond to taking the derivative of the total energy with a fixed number of plane waves in the basis set. Because of this our calculated stresses are not close to zero; in fact for the $\langle\infty\rangle$ phase at the experimental lattice constant we obtain a pressure of about -142 kbar, where the negative sign indicates that an expansive pressure must be exerted to keep the structure at this lattice constant. Our method was to relax the structures of the other polytypes until there were no forces on the atoms and the stress tensor was identical to that calculated for the $\langle\infty\rangle$ phase. This was done by moving the atoms and changing the size and shape of the unit cell in the directions indicated by the calculated forces and stresses.

We have used a basis set containing all plane waves with kinetic energy less than a cut-off value of 32 Ryd. Integrations over the Brillouin zone were performed by a special points technique using the scheme of Monkhorst and Pack [16]. For the $\langle 1\rangle$, $\langle\infty\rangle$, $\langle 2\rangle$ and $\langle 3\rangle$ polytypes we used a hexagonal unit cell and exactly equivalent sets of special points corresponding to sampling 12 k-points in the irreducible wedge of the Brillouin zone of the $\langle 3\rangle$ structure. For the calculations on the polytype $\langle 23\rangle$ we used a rhombohedral unit cell and a special points set consisting of 57 points within the irreducible wedge. When comparing total energies it is important to use exactly equivalent Brillouin zone integrations, as explained in [2]. Thus we are able to compare directly the energies of the $\langle 1\rangle$, $\langle\infty\rangle$, $\langle 2\rangle$ and $\langle 3\rangle$ polytypes with one another but not with the $\langle 23\rangle$ polytype. However, we are able to calculate the relaxation energy of the $\langle 23\rangle$ polytype because this is the energy difference between the ideal and relaxed structures that are both calculated in the rhombohedral unit cell. Note the rather large number of k-points sampled and the way they are chosen to be exactly equivalent for all except the $\langle 23\rangle$ structure. We estimate that the error in the energy differences between structures due to the finite sampling used for the Brillouin zone integrations is less than 0.001 eV per unit cell.

For calculating the energy difference of two slightly different structures it is important to minimise the error due to the use of a truncated basis set [17]. As we have already mentioned, this is best done by keeping the basis set energy cut-off fixed when changing the volume of the system by large amounts. However, when considering very small strains of the unit cell, as in relaxing the polytype structures, it is much better to keep the number of plane waves in the basis set constant. This procedure eliminates jumps in

Table 1. Calculated stresses of the polytypes before and after relaxation (in units of 10^9 dyn cm^{-2}). The small difference between the longitudinal and transverse stresses of the cubic ⟨∞⟩ structure are due to the lack of cubic symmetry of the k-points used. We used a hexagonal unit cell for the ⟨∞⟩ structure such that exactly the same k-points could be used for all the structures (except ⟨23⟩).

Stress	⟨∞⟩	⟨1⟩	⟨2⟩	⟨23⟩	⟨3⟩
Ideal structure					
σ_{xx}	−142.455	−152.689	−148.507	−147.530	−146.408
σ_{zz}	−142.462	−118.694	−131.694	−133.876	−135.292
Relaxed structure					
σ_{xx}		−142.568	−142.639	−142.515	−142.679
σ_{zz}		−142.611	−142.539	−142.537	−142.476

the total energy, which would result from the changes in the size of the basis set if the plane-wave cut-off energy were kept fixed.

Let us first define the relaxation energy E_r that we want. We start with the cubic ⟨∞⟩ structure at *its* equilibrium volume $V_{c,m}$ at pressure $P = 0$, where suffix c denotes the cubic phase and m denotes the condition of minimum energy U. We construct the 'ideal' polytype (suffix i) with ideal tetrahedral angles and bond lengths equal to that of the cubic structure, i.e. $V_i = V_{c,m}$. It will not be at zero pressure but will relax in volume, c/a ratio and internal coordinates to give the relaxed polytype (suffix r) at its equilibrium volume $V_{r,m}$ at $P = 0$. The relaxation energy is defined as

$$E_e = U_r(P = 0) - U_i(V_{c,m}). \tag{2.1}$$

There are three problems about calculating the relaxation energy (2.1). The first is that it is so small, of order 1 meV per SiC pair of atoms, and the difference Δ_r (1.4) that we want is measured in μeV per SiC pair. Secondly, in our calculations we choose to work at some non-zero pressure P_0 at which our computed *cubic* phase has the volume V_0 (which was chosen as the experimental equilibrium volume of the cubic phase at $P = 0$, but that is immaterial here). However, the energies of the relaxed structures that have different volumes *and* are under finite pressure should not be compared with each other, and we have to apply a correction accordingly. In effect we want an enthalpy difference rather than the energy difference. Thirdly, we do not know what P_0 is, corresponding to our chosen cubic V_0, because the absolute pressure is a slowly convergent quantity. With a cut-off of 32 Ryd, we have a pressure of −142 kbar (table 1), but we estimate that the converged value may be about half of this. However, we trust that differences in the calculated stresses are significant between the various polytypes, for which one can see evidence in the systematic trends of table 1. We would point out that the accuracy of energy differences in total-energy calculations is usually considered to be of order 1 meV: even to talk in terms of μeV is pushing the calculation well beyond what is normal. Thus the three problems above are more significant in our case than they would usually be.

We have considered various ways of dealing with these three problems, and believe the following is the most 'robust' in the sense of being least sensitive to noise and convergence error. For a simple spring, the energy, from equilibrium, can be written as

$(1/2)Fx$, where F is the final force $F = \lambda x$ when the extension is x. Consider now a system acted on by forces F_i producing displacements x_i where $F_i = \Sigma\lambda_{ij}x_j$. The total energy is

$$E = (1/2)\sum_i F_i x_i \tag{2.2}$$

as can be seen by 'turning on' all the forces uniformly and simultaneously: there is no assumption about λ_{ij} being diagonal, only elastic linearity. The necessary and sufficient condition is that F_i be given by

$$F_i = (\partial E/\partial x_i) \qquad \text{with all other } x_j = \text{constant}. \tag{2.3}$$

In our case, let us start from the relaxed structure at equilibrium and apply forces and stresses to bring it to the ideal structure (with cubic bond lengths and bond angles). The energy is then given by (2.2), and the relaxation energy in the sense of (2.1) is the negative of it, i.e.

$$E_r = -(1/2)\sum F_i x_i. \tag{2.4}$$

It remains to define the F_i and x_i more precisely. There are three contributions

$$E_r = E_r^i + E_r^a + E_r^c \tag{2.5}$$

where superscripts i, a and c refer respectively to the internal coordinates within the unit cell and to the relaxation of the a and c lattice parameters. For the 'external' displacement x_c we have $x_c = \delta c$, the change in the c lattice parameter. The corresponding F_c is the stress σ_{zz} in the ideal structure multiplied by the area of the 'top' of the unit cell. With slight rearrangement we have

$$E_r^c = -(1/2)V\sigma_{zz}\delta c/c \tag{2.6}$$

where V is the volume of the unit cell. For the other 'external' displacement $x_z = \delta a$ we have to combine the (equal) stress σ_{xx} and σ_{yy} to obtain

$$E_r^a = -(1/2)V\sigma_{xx}\delta a/a. \tag{2.7}$$

The internal forces F_i with $i = 1$ to n are the Hellmann–Feynman forces f_i on the n atomic layers in the unit cell. By symmetry, they are all in the z direction. Let z_i be the position coordinate of the ith layer in the usual crystallographic sense, i.e. in units of the cell height c, measured from some chosen origin. Then the 'internal' displacement coordinate x_i is $c\delta z_i$. Note that, in order to satisfy (2.3), it is not $\delta(cz_i)$. Thus we have

$$E_r^i = -(1/2)\sum f_i c\delta z_i. \tag{2.8}$$

This formula is invariant, as it should be, under a shift in the origin from which the z_i are measured because the Hellmann–Feynman forces sum to zero. Note (2.6) to (2.8) are given per unit cell, not per SiC pair of atoms. In our case the stresses σ_{xx} and σ_{yy} are to be interpreted as the differences from P_0, or to be precise from the reference stresses of the cubic structure in table 1. Thus (2.6) to (2.8) constitute our method for calculating the relaxation energy. We like it for two reasons. First, it is expressed in terms of quantities σ_{zz}, δc, f_i, δz_i, etc., that are linear in the relaxation, whereas the total energy being very large but quadratic in the relaxation is in our experience more susceptible to numerical error. Secondly, in our method cancelling out the pressure P_0 is effected in an analytic way when defining the σ_{zz}, etc., to be inserted in (2.6) and (2.7), whereas it

Table 2. The ion–ion contribution, electron–ion contribution, total atomic forces and the modulus of the sum of the forces on the Si or C atoms for ideal polytypes (in units of 10^{-3} dyn). The f_i are defined in figures 1 to 4.

Structure	$f_{\text{ion-ion}}$	$f_{\text{elec-ion}}$	f_{total}	$\lvert F(\text{Si})\rvert = \lvert F(\text{C})\rvert$
⟨1⟩ f_1	0.1543	−0.1769	−0.0226	0.0226
f_2	−0.1543	0.1769	0.0226	
⟨2⟩ f_1	−0.0004	−0.0096	−0.0100	0.0250
f_2	−0.1543	0.1502	−0.0041	
f_3	0.1543	−0.1693	−0.0150	
f_4	0.0004	0.0287	0.0291	
⟨3⟩ f_1	0.0000	−0.0076	−0.0076	0.0257
f_2	−0.1562	0.1512	−0.0050	
f_3	−0.0023	−0.0064	−0.0087	
f_4	0.0023	0.0034	0.0057	
f_5	0.1562	−0.1656	−0.0094	
f_6	0.0000	0.0250	0.0250	
⟨23⟩ f_1	−0.0004	−0.0075	−0.0079	0.02545
f_2	−0.1543	0.1479	−0.0064	
f_3	0.1543	−0.1672	−0.0129	
f_4	0.0004	0.0268	0.0272	
f_5	0.0000	−0.0089	−0.0089	
f_6	−0.1562	0.1530	−0.0032	
f_7	−0.0023	−0.0081	−0.0104	
f_8	0.0023	0.0049	0.0072	
f_9	0.1562	−0.1670	−0.0108	
f_{10}	0.0000	0.0261	0.0261	

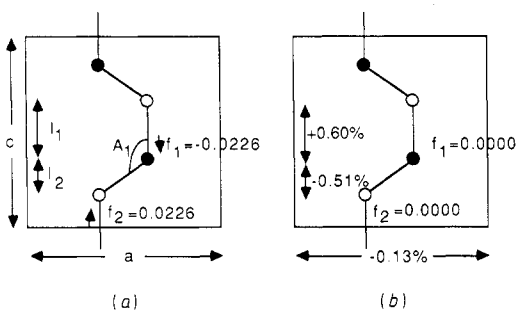

Figure 1. The unit cells of (*a*) the ideal and (*b*) the relaxed ⟨1⟩ structures. The full circles indicate Si atoms while the open circles indicate C atoms. In (*a*) the angles A_i, interlayer spacings l_i (between single atomic layers) and Hellmann–Feynman forces f_i are defined, and the values of f_i in the ideal structure in 10^{-3} dyn given. In (*b*) the percentage changes due to the relaxation in the intervals l_i are given, and the residual f_i when the calculation was stopped.

is a large numerical correction when one works with the total energy as given by the electronic structure.

3. Atomic forces and stresses in the ideal structures

In this section we shall, first, analyse the calculated atomic forces of the four polytypes, i.e. ⟨1⟩, ⟨2⟩, ⟨3⟩ and ⟨23⟩, in their ideal structures to derive the force field produced by an

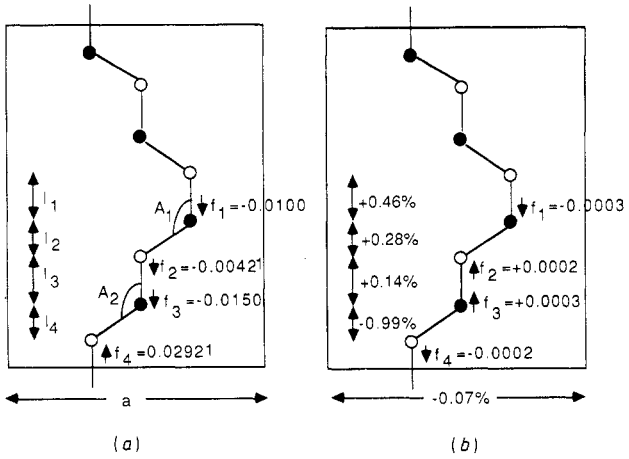

Figure 2. The unit cells of the ideal and relaxed ⟨2⟩ structures. See caption of figure 1 for explanation.

isolated boundary. Secondly, we connect the calculated forces and stresses by our simplified tension model.

The atomic forces and the residual stresses (taking the isotropic stress of ⟨∞⟩ as the reference) in the ideal structures may be regarded as due to the presence of boundaries. The forces on the atoms in the cubic ⟨∞⟩ phase are zero by symmetry. For other polytypes, the forces on the atoms may be non-zero only along the stacking direction (z axis). The ⟨∞⟩ structure has only a single parameter that is not determined by symmetry, the lattice constant, and consequently the stress tensor must be a multiple of the identity matrix. All other polytypes have two independent components of the stress tensor, σ_{zz} in the stacking direction and $\sigma_{xx} = \sigma_{yy}$ in the plane of the layers. The values of the stress components and the forces are listed in tables 1 and 2 and figures 1 to 4. The residual stresses are larger, as expected, for structures with a smaller value of the mean band width, i.e. a larger concentration of boundaries. However, the pattern of the forces is puzzling and not easy to understand at first sight. For example, the forces in ⟨1⟩ are not as strong as f_4 in ⟨2⟩ or f_6 in ⟨3⟩, and why are the strongest forces f_4 in ⟨2⟩, f_6 in ⟨3⟩ and f_4 and f_{10} in ⟨23⟩?

To have a better understanding of the forces, we decompose them into two parts. One is the ion–ion contribution, where Si and C are treated as identical ions with charge $+4\,|e|$ placed in a neutralising background with uniform electron charge density. The other is the electron–ion contribution, which depends on the type of atom. These two contributions for the structures ⟨1⟩, ⟨2⟩, ⟨3⟩ and ⟨23⟩ are listed in table 2. The atoms that experience the strongest forces are not those closest to the centre of the boundary but those removed one atom spacing from them, namely C(0) and Si(0) in figure 5. One also notices that the ion–ion contributions in ⟨23⟩ are the same as those of ⟨2⟩ and ⟨3⟩, which shows that the ion–ion contribution is short-ranged, i.e. extending only to nearest-neighbour boundaries.

Now we deduce the force pattern formed by the presence of an isolated boundary. As mentioned in section 1, the force fields of two boundaries will overlap if the two boundaries are close enough to each other. We say the effect of boundaries is additive if the force fields produced by all boundaries are the same and are simply additive. We

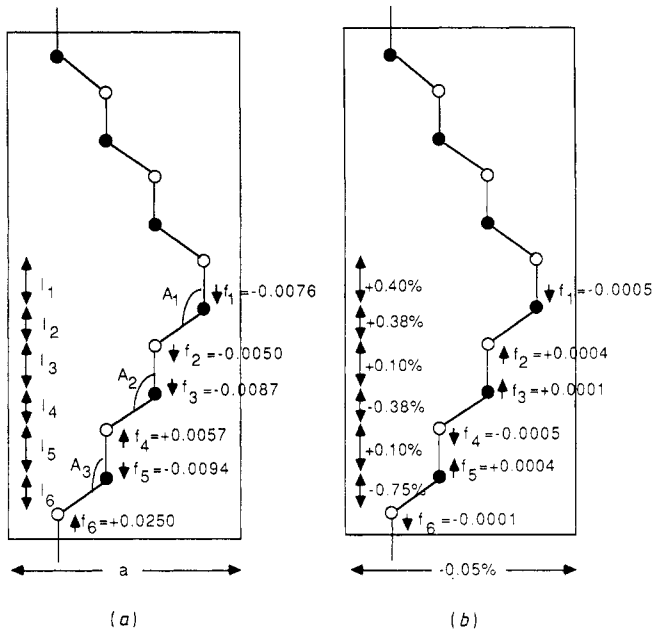

Figure 3. The unit cells of the ideal and relaxed ⟨3⟩ structures. See caption of figure 1 for explanation.

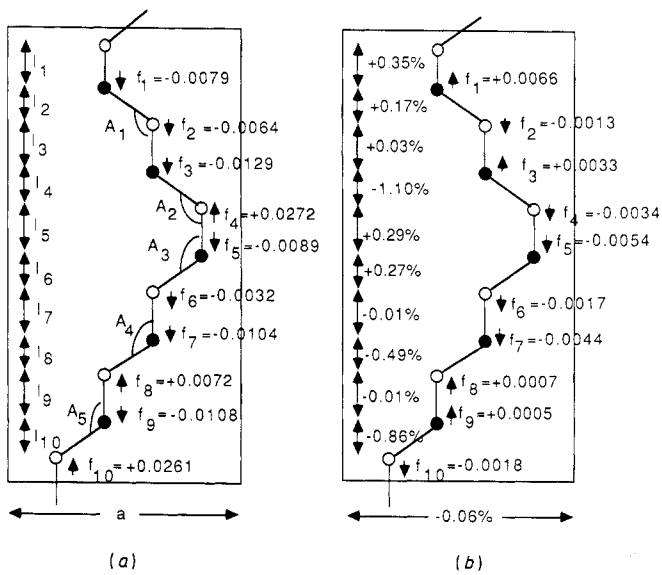

Figure 4. The unit cells of the ideal and relaxed ⟨23⟩ structures. See caption of figure 1 for explanation.

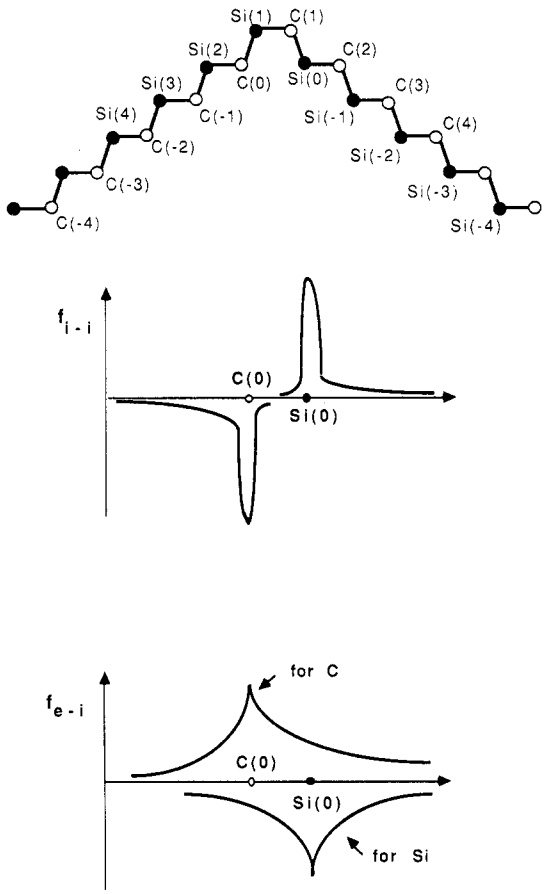

Figure 5. Schematic diagram showing the force field resulting from an isolated boundary. The full circles are Si atoms and the open circles C atoms.

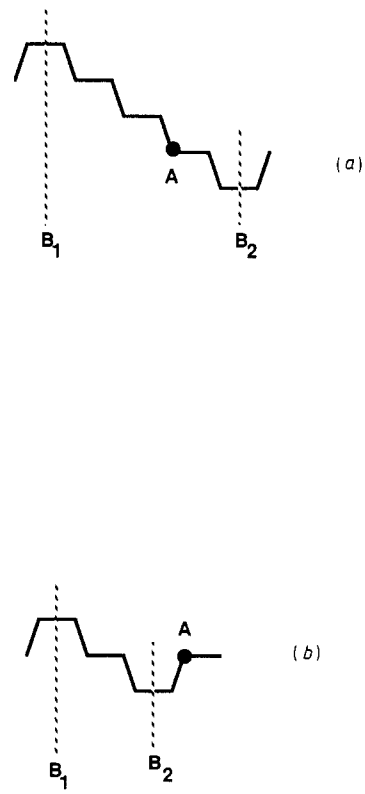

Figure 6. Schematic picture of one chain of atoms in the polytypes with antiphase boundaries (see text). In both (*a*) and (*b*) atom A is the sixth atom removed from the centre of the boundary B_1.

may expect additivity from linear response theory for the forces on atom A due to boundaries B_1 and B_2 in the case of figure 6(*a*). However, there is no reason for additivity to hold rigorously in the geometry of figure 6(*b*), where the force on the atom A due to the boundary B_1 may be affected by the intervening boundary B_2, which alters the position of the atom relative to B_1 (cf. figure 6(*a*)). We can test how well additivity holds as follows. The sum of the f_i in a structure has to be zero, and hence the partial sums

$$F(\mathrm{Si}) = \sum_i f_i(\mathrm{Si}) \qquad F(\mathrm{C}) = \sum_i f_i(\mathrm{C}) \tag{3.1}$$

for silicon and carbon atoms have to be equal and opposite. If the additivity property holds, then the partial sums per boundary should be the same in all structures. The quantities (3.1) per boundary are listed in table 2. For polytypes ⟨2⟩, ⟨3⟩ and ⟨23⟩ the non-additivity is only 3% of the total forces per boundary, while for ⟨1⟩, compared with the above three, the non-additivity is about 14%. Therefore, having checked the additivity, we can evaluate the force field from a single boundary from the calculated

Table 3. The electron–ion contribution to atomic forces (in 10^{-3} dyn) for an isolated boundary on atoms X(i) where X = Si or C, as defined in figure 5.

Atom	X(0)	X(1)	X(−1)	X(2)	X(−2)	X(3)	X(−3)	X(4)	X(−4)
Si	−0.1623	−0.0038	−0.0028	−0.0031	−0.0032	−0.0014	−0.0018	−0.0004	−0.0004
C	0.1483	0.0209	0.0052	−0.0025	0.0039	0.0007	0.0020	0.0001	0.0005

forces of ⟨2⟩, ⟨3⟩ and ⟨23⟩. We make a least-squares fit to the electron–ion contribution to the forces in ⟨2⟩, ⟨3⟩ and ⟨23⟩ and obtain the force field of an isolated boundary shown in table 3 and schematically in figure 5. For both the Si and C atoms, the force field extends to the fourth-neighbour atom, but only with a tiny value that is of the same order of magnitude as or less than the non-additivity. The ion–ion contribution, as mentioned above, is short-ranged and can be read off from table 2. It is more or less like a delta function on the second atoms from the centre of a boundary (Si(0) and C(0) in figure 5). We thus conclude that the range of the force field of a boundary is up to third-neighbour atomic double layer with only tiny tails extending beyond that. The electron–ion force field on C atoms is more anisotropic than that on Si atoms (figure 5). The total force on an atom is therefore expected to be in the same direction as that of the electron–ion contribution except for Si(0) and C(0), where it is determined by the two large values of the ion–ion and electron–ion contributions. The force field also explains the strongest forces f_4 in ⟨2⟩, f_6 in ⟨3⟩ and f_4 and f_{10} in ⟨23⟩. These strongest forces are formed on the atoms where the ion–ion forces are already very small and the electron–ion forces are still strong. What is not clear to us is why the decomposed forces in figure 5 are centred on atoms C(0) and Si(0), one removed from the centre of the boundary, rather than on C(1) and Si(1) directly beside the boundary.

We now discuss the significance of additivity and non-additivity on the BBI. Obviously the additive part of the force field gives a BBI (I_m) that does not depend on the presence of another boundary and thus we have $I_m^{\mathrm{NN}} = I_m^{\mathrm{NNN}}$. We expect this relation to hold well, as the non-additive part is only a small proportion of the force field. Note that this is very different from the BBI of the phonon free energy in paper I, where the leading terms in I_m^{NN} and I_m^{NNN} have opposite signs.

In the second half of this section we propose a grossly simplified tension model to connect both the macroscopic stresses $\sigma_{xx} = \sigma_{yy}$, σ_{zz} and the atomic forces f_i in the ideal structures. The atomic bonds of polytypes are modelled as springs with tensions to account for both the atomic forces and the stresses. Consider a polytype with n non-equivalent bonds per repeating unit under tension T_i with $i = 1$ to n. These have to be fitted to the $n + 2$ quantities, namely the n forces f_i and two stresses σ_{xx} and σ_{zz}. However, the f_i have to sum to zero, so that only $n + 1$ forces and stresses are independent. Thus the tension model is overdetermined and we therefore include an extra fudge factor α, which will also serve to indicate how good the model is. For example, in the structure ⟨1⟩, the three equations to give the tensions T_1 and T_2 (T_i corresponds to the tension of bond b_i in figure 1) are

$$\sigma_{zz}A_{zz} = (\alpha/4)(3T_1 + T_2) \tag{3.2}$$

$$\sigma_{xx}A_{xx} = \alpha(\sqrt{8}/3)T_2 \tag{3.3}$$

$$f_1 = T_1 - T_2 \tag{3.4}$$

Table 4. The evaluated tensions, parameter α and relaxation energies (equation (3.5)) of the tension model using the atomic forces and stresses of the ideal structures. The tensions T_i are in units of 10^{-3} dyn corresponding to the bonds in the intervals l_i defined in figures 1 to 4. The relaxation energies are in units of 10^{-4} eV per SiC pair. The corresponding percentage (%) changes of the bond lengths estimated from equation (3.6) and the T_i are given in parentheses.

	⟨1⟩	⟨2⟩	⟨23⟩	⟨3⟩
$E_r(3.5)$	−7.089	−8.132	−6.235	−4.984
α	1.65	1.48	1.47	1.44
T_1	0.0175 (0.55)	0.0162 (0.51)	0.0157 (0.49)	0.0156 (0.49)
T_2	−0.0051 (−0.16)	0.0062 (0.19)	0.0078 (0.24)	0.0080 (0.25)
T_3		0.0020 (0.06)	0.0014 (0.04)	0.0030 (0.09)
T_4		−0.0129 (−0.40)	−0.0115 (−0.36)	−0.0057 (−0.18)
T_5			0.0157 (0.49)	0.0000 (0.00)
T_6			0.0068 (0.21)	−0.0094 (−0.29)
T_7			0.0036 (0.11)	
T_8			−0.0068 (−0.21)	
T_9			0.0004 (0.01)	
T_{10}			−0.0104 (−0.33)	

where A_{zz} and A_{xx} are the areas of the unit cell with normal vector perpendicular and parallel to the stacking plane and the numerical factors come from the direction cosines. The fitted tensions in the atomic bonds for the four polytypes have been determined from analogous equations and are listed in table 4. Note that $\alpha = 1$ corresponds to a perfect fit of the model to the calculated forces and stresses. However, the values of α for ⟨2⟩, ⟨3⟩ and ⟨23⟩ range from 1.44 to 1.48. For ⟨1⟩, the α is 1.65. This is due to idealising the stress in an atomic bond by a simple spring, and neglecting the bond-bending forces. The very different value of α for ⟨1⟩ is the effect of non-additivity when compared to ⟨2⟩, ⟨3⟩ and ⟨23⟩.

We get several things from this simplified model. First, the fact that α is nearly constant and of order unity connects the origin of the macroscopic stresses and their signs with the internal forces. We have a picture in which the bonds have an internal tension, wanting to expand or contract. Where these internal tensions come from will be interpreted in the next section. Secondly, we have a rough estimate of the relaxation energy per unit cell

$$E_r = -\sum_i [T_i^2/(2\lambda)] \tag{3.5}$$

where the sum is over all bonds in a unit cell and λ is the force constant of stretching a Si–C bond. Equation (3.5) is a simplified form of (2.4) to (2.7). We obtain the value of λ from the bulk modulus of ⟨∞⟩ structure [18]. The relaxation energies calculated from (3.5) are listed in table 4. Thirdly, equation (3.5) shows immediately the origin of the BBI. Since the equations analogous to (3.2) to (3.4) for the different polytypes are all linear, the additivity of forces f_i translates into additivity of tensions T_i. However the energy (3.5) is quadratic in the T_i so that the total energy is sensitive to the relative sign

Table 5. The percentage differences of the lattice constants, unit cell volume V and internal structure parameters of the relaxed structures from the ideal ones. The A_i relate to the bond angles and b_i the bond lengths in the regions l_i defined in figures 1 to 4. The numbers in parentheses are from experiment ([19] for ⟨1⟩ and [20] for ⟨3⟩).

Structure parameters	⟨1⟩	⟨2⟩	⟨23⟩	⟨3⟩
c	0.319 (0.278)	0.136	0.108	0.090 (0.102)
a	−0.133 (−0.217)	−0.075	−0.062	−0.050 (−0.068)
V	0.053 (−0.163)	−0.013	−0.017	−0.010 (−0.033)
A_1	−0.062	0.059	0.056	0.070
A_2		−0.150	−0.150	−0.054
A_3			0.072	−0.115
A_4			−0.053	
A_5			−0.114	
b_1	0.595	0.460	0.460	0.404 (0.33)
b_2	−0.144	−0.051	−0.022	−0.023 (−0.09)
b_3		0.138	0.140	0.104 (0.33)
b_4		−0.121	−0.161	−0.066 (−0.14)
b_5			0.400	0.102 (0.17)
b_6			−0.011	−0.086 (−0.09)
b_7			0.100	
b_8			−0.096	
b_9			0.100	
b_{10}			−0.136	

(cancellation or enhancement) of the contributions T_{i1} and T_{i2} from nearby boundaries 1 and 2. Fourthly, the changes in bond lengths b_i would be

$$\delta b_i = T_i/\lambda \tag{3.6}$$

(also listed in table 4). Comparison of the estimates (3.6) of the changes in bond lengths from table 4 with the results of the proper relaxation calculations in table 5 shows qualitative agreement. The interpretation is not so good for some diagonal bonds because the bond-bending forces are not taken into account. In the structures ⟨2⟩, ⟨3⟩ and ⟨23⟩, where the transverse strain (discussed in section 1) is present, the inclusion of the bond-bending forces and the constraint of a constant lattice a for every layer in a structure is particularly important. This explains why the comparison is best for the ⟨1⟩ structure, where there is no transverse strain in the ⟨1⟩ structure of the type discussed in section 1. Note that the relaxations are related to the tensions, and not directly to the forces f_i. The latter point is obvious from considering the case where neighbouring atomic layers happen to have the same f_i: presumably both will relax by the same amount in the same direction so that there is zero change in the bond length between them. It is therefore necessary to use something like our tension model to extract physically significant information from the f_i.

4. Results of the relaxation calculations: the relaxed structures

The results of the relaxation are shown in table 5 and in figures 1 to 4. The ⟨1⟩, ⟨2⟩ and ⟨3⟩ polytypes were relaxed until the forces were of the order of 10^{-7} dyn and in each case

the components of the stress tensor were different from those of the ⟨∞⟩ structure by less than 0.15% (table 1). The ⟨23⟩ polytype was not as fully relaxed as the other three polytypes.

The deviations in the average separation l_i between layers in the z direction, c, and the spacing a within the layers from the ideal values increase monotonically with increasing concentration of boundaries in the polytype, especially for structures ⟨2⟩, ⟨3⟩ and ⟨23⟩. Note that the spacings l_i relate to actual atomic layers of Si or C, whereas the word 'layer' elsewhere refers to a SiC double atomic layer. The greater the concentration of boundaries, the larger the value of c and the smaller the value of a. This is the same trend as shown by the stresses of the ideal structures (table 1). However, the changes in volume are more irregular. Our calculated volume change for the ⟨1⟩ polytype is opposite in sign to the reported experimental result [19]. Experimentally the volume of the ⟨1⟩ polytype is 0.16% smaller than that of the ⟨∞⟩ polytype, while our calculations give a volume 0.053% larger than the ⟨∞⟩ polytype. One possible explanation of this disagreement is that the specimens may have been far from perfect because the ⟨1⟩ polytype is almost certainly not thermodynamically stable and is formed under rather special growth conditions. Besides, the volume of a structure can easily be affected by the presence of impurities. We therefore suggest that it would be interesting if the measurements could be repeated on samples with greater chemical and structural perfection or with the same impurities in ⟨1⟩ and ⟨∞⟩. Another possible origin of the discrepancy is the use of the incomplete basis set or the local density approximation in our calculations. However, from general experience with such calculations, we do not think these are significant effects. We also note that the structure ⟨23⟩ has a smaller relaxed volume than those of ⟨2⟩ and ⟨3⟩. This is because the stress σ_{xx} and the δa of ⟨23⟩ (with $x = 2/5$ in the sense of equation (1.2)) do not interpolate linearly between those of ⟨2⟩ and ⟨3⟩ with $x = 1/2$ and $1/3$, respectively. This is probably an artifact because we had to use a rhombohedral unit cell and corresponding set of k-points for ⟨23⟩ that are different from those for the other polytypes.

The most interesting aspect of the relaxations is that the percentage changes in bond angles are small compared with those in the bond lengths (table 5). This was also observed by Gomes de Mesquita [20], who determined the detailed structure of ⟨3⟩ using x-ray diffraction. The measured relaxations are included in table 5 and seen to be in reasonable qualitative agreement with our calculated ones. It must be remembered that we are dealing with effects at the very limit of accuracy of this type of calculation. The bond-angle changes calculated from the measured changes in interlayer spacing are all less than 0.12%. Note that the sign of our calculated volume relaxation agrees with the observed sign in this case. The agreement between calculation and experiment for ⟨3⟩ validates the general trends in our calculations, which in turn suggests that the smallness of the bond-angle relaxations is a general feature of the SiC polytypes as found in all our calculations. The smallness of the bond-angle change is particularly noticeable in the ⟨1⟩ structure, where the bond-length change and the density of boundaries is largest. The phenomenon is at first sight surprising because bond-bending force constants are weaker than bond-stretching ones, leading in amorphous Si, for example, to a wider distribution of bond angles than of bond lengths. We offer the following explanation. The analogy with amorphous Si is beside the point: there and elsewhere the small bond-bending force constant leads to larger bond-angle changes in response to *external* forces or constraints. Here we are dealing with internal differences in electronic structure between the bonds due to differences in the geometrical environment. One has different amounts of sp hybridisation and different degrees of bonding. Although one might picture the diamond

Table 6. The three contributions (2.6) to (2.8) to the relaxation energy $E_r(2.4)$, and corresponding contributions to $\Delta_r(5.1)$, all in 10^{-6} eV per SiC pair of atoms. The last line gives the same E_r per boundary (p.b.).

	⟨1⟩	⟨2⟩	⟨23⟩	⟨3⟩	Δ_r
E_r^c	−491	−95	−60	−42	3
E_r^a	−173	−57	−40	−24	−3
E_r^i	−367	−307	−229	−181	2
$E_r(2.5)$	−1031	−459	−329	−247	2
E_r(p.b.)	−1031	−917	−823	−740	—

Table 7. The calculated energies of ideal [2] and relaxed structures, and the relaxation energies of the polytypes defined in other ways, in eV per SiC pair.

	⟨1⟩	⟨2⟩	⟨23⟩	⟨3⟩
Ideal	−263.07538	−263.08486	−263.08456	−263.08526
Relaxed	−263.07539	−263.08554	−263.08519	−263.08566
$E_r(4.1)$	−0.000054	−0.000662	−0.000611	−0.000385
$H_r(4.3)$	−0.00098	−0.00044	−0.00032	−0.00022

structure as consisting of purely bonding orbitals between perfect sp^3 hybridised directed valence orbitals, the reality that emerges from a tight-binding analysis of the electronic band structure is rather different [21]. In particular, the configuration $s^x p^{4-x}$ for silicon has $x \simeq 1.3$. Paxton [22] has made calculations for silicon in the structure ⟨1⟩ and found a higher total bond order for the diagonal bonds than for those parallel to the c axis. The former will therefore 'want' to be shorter than the latter, in agreement with relaxation calculations on ⟨1⟩ SiC (table 5 and figure 1). In the ⟨1⟩ structure, the two types of bond can have different lengths while still retaining the perfect tetrahedral bond angles. That presumably still optimises satisfying the exclusion principle, as can be seen in molecules like CH_3Cl where the bond angles are still near perfect while the bonds to H and Cl are quite different. We suggest this as the explanation for the small bond-angle changes in ⟨1⟩ SiC. In the other polytypes it is geometrically not possible to retain perfect tetrahedral bond angles while having differences in bond lengths because the a lattice constant of all the atomic layers is constrained to be the same. Thus larger relaxations of bond angles are found in the polytypes ⟨2⟩, ⟨23⟩ and ⟨23⟩ (table 5) as a result of bond-length changes.

We turn now to the relaxation energy E_r (2.4) to (2.8), the various contributions and the total being given in table 6. The last line of the table gives the relaxation energy per boundary (p.b.). It is very nearly constant: the deviation of E_r(p.b.) from a constant is due to the BBI with nearest-neighbour boundaries, which is clearly significant.

We have tried other ways of formulating E_r as mentioned in section 2. If we assume that the bulk modulus B is the same for the relaxed (B_r) and ideal (B_i) polytypes and the cubic phase (B_c), then we can correct for the pressure P_0 to derive the result

$$E_r = U_r(P = P_0) - U_i(V_0) - P_0[P_0 - P_i(V_0)]/B \tag{4.1}$$

where $P_i(V_0)$ is the calculated stress for the ideal polytype structures at volume V_0. The values are given in table 7 using the bulk modulus from experiment [18]. They are clearly

disastrous, the structure ⟨1⟩ with the greatest number of boundaries having by far the smallest relaxation energy. However, if the bulk moduli are not equal, there is a further correction

$$(P_0/B_c)P_0[1 - (1/2)(B_i/B_c) - (1/2)(B_c/B_r)]. \tag{4.2}$$

We find that a 0.2% difference between the three B_γ can give a correction of similar magnitude to the original correction term in (4.1). Therefore, the additional term (4.2) cannot be ruled out. Furthermore, there is some evidence in our calculations that the convergence error in the pressure is not the same for all the structures, another of our assumptions.

A better approach to the relaxation energy is the relaxation enthalpy at pressure P_0,

$$H_r = [U_r(P_0) - U_i(V_0)] + P_0(V_r - V_0). \tag{4.3}$$

This is the correct definition of the relaxation 'energy' under two conditions. (i) The process of relaxation is carried out in an environment of constant pressure $P = P_0$ instead of $P = 0$ (cf. equation (2.1)). The quantity (4.3) is necessarily negative, is quadratic in the sense that linear terms due to change of volume are subtracted out by the last term of (4.3), and there is no attempted extrapolation from P_0 to $P = 0$. (ii) The energy is governed by calculations with a constant number of plane waves in the basis set. Note that our formula for evaluating the stress is analytically the differential of the energy with a fixed number of plane waves. Thus there is analytic consistency in the cancellation of first-order contributions between the two terms of (4.3). The H_r is equivalent to (2.5) to (2.8) if we use for σ_{zz} and σ_{xx} in (2.6) and (2.7) the deviation of the stresses from P_0, as we have done in table 6. The H_r calculated from (4.3) are given in table 7 and agree with the results of table 6 apart from differences in the last significant figure of table 7. This is gratifying, but clearly the formulation (2.4) is superior because it is analytically quadratic in the relaxation whereas in (4.3) there is a numerical cancellation between substantial linear terms.

5. The stability of ⟨23⟩ polytype due to relaxations

The most important part of the present work is to calculate the role of structural relaxation for the stability or instability of the polytype ⟨23⟩ as an intermediate phase between ⟨2⟩ and ⟨3⟩ in the sense of paper I. We define the relaxation contribution Δ_r to Δ in accordance with (1.1) by

$$\Delta_r = E_{r\langle 23\rangle} - (2/5)E_{r\langle 2\rangle} - (3/5)E_{r\langle 3\rangle} \tag{5.1}$$

where all energies are expressed per SiC pair of atoms. Table 6 includes the contributions to Δ_r from the three parts (2.6) to (2.8) of E_r and the total. It is very small, of order 2×10^{-6} eV per SiC pair. From (5.1), it is determined by the deviation of E_r from linear dependence on the concentration of boundaries in ⟨2⟩, ⟨23⟩ and ⟨3⟩. This is very small because indeed the structure ⟨23⟩ is very close to being a sandwich of a 2-band from ⟨2⟩ and 3-band from ⟨3⟩, as we have already seen in all the trends of tables 1, 2, 4 and 5 and figures 2 to 4. An alternative view is to note from (1.4) that Δ_r is related to the BBI to the second-neighbour boundaries, and from the discussion of table 3 and figure 5 the stress field generated by a boundary is small at those distances. Even then, there are cancellations in I_m: since the f_i from a boundary must sum to zero, there are cancelling positive and negative overlap terms with the neighbouring boundary. On top of that

there are further cancellations expected among the three terms in (1.4). It is therefore not surprising that Δ_r is of order 1% of E_r. Incidentally we get an even smaller Δ_r from the use of (3.5) and (5.1). It is somewhat surprising that the contribution Δ_r^a of the δa relaxation is negative (table 6). We would expect it to be positive from the discussion of section 1. This is probably due to the (necessary) use of a different k-point sample for $\langle 23 \rangle$ from that for $\langle 1 \rangle$, $\langle 2 \rangle$, $\langle 3 \rangle$ and $\langle \infty \rangle$, so that the calculated stress σ_{xx} of $\langle 23 \rangle$ does not interpolate nicely between that of $\langle 2 \rangle$ and $\langle 3 \rangle$ in the ideal structures. Let us see what it is assuming linear interpolation by writing

$$\delta a/a = -(0.15/L) \text{ per cent} \qquad \sigma_{xx} = -(12/L) \times 10^9 \text{ dyn cm}^{-2} \tag{5.2}$$

where L is the number of atomic double layers per boundary, i.e. 2, 5/2 and 3 for our polytypes, and where σ_{xx} is the deviation from the value for $\langle \infty \rangle$ in table 1. The fact that (4.1) even fits the calculated σ_{xx} and δa for the structure $\langle 1 \rangle$ argues strongly that linearity should apply to $\langle 23 \rangle$. The calculation of E_r^a from (2.5) and (5.2) converted to energy per SiC pair of atoms and then inserted in (5.1) gives $\Delta_r^a = 1.5 \times 10^{-6}$ eV per SiC pair, which is positive as it should be in accordance with section 1. This indicates the likely uncertainty in our final Δ_r, which is otherwise difficult to estimate. We hesitate to 'correct' this one contribution to Δ_r in table 6, fearing to destroy any cancellation of errors inherent in the whole of the calculation. The indication is, as already stated, that $\langle 23 \rangle$ is a better interpolation between $\langle 2 \rangle$ and $\langle 3 \rangle$ than is evident in our calculation because of the difference in k-point sampling. Any greater similarity of $\langle 23 \rangle$ to $\langle 2 \rangle$ and $\langle 3 \rangle$ will reduce Δ_r^c and Δ_r^i, leaving in the limit only the Δ_r^a given above.

We therefore take

$$\Delta_r = 2 \times 10^{-6} \text{ eV per SiC pair} \tag{5.3}$$

as our final best estimate of Δ_r, with an uncertainty of at least 100%. However, the uncertainty would have been an order of magnitude greater without the use of our formulation (2.4) to (2.8). The Δ_r (5.3) has to be compared with $\Delta_{ph} = -4 \times 10^{-6}$ eV per SiC pair from the phonon free energy at the relevant temperature (around 2400 K) as calculated in paper I. The negative sign of Δ_{ph} would make $\langle 23 \rangle$ a stable intermediate phase between $\langle 2 \rangle$ and $\langle 3 \rangle$. All we can really say is that Δ_r is likely to be small enough not to wipe out $\langle 23 \rangle$ as an intermediate phase, though it probably will reduce the stability range considerably from the estimate of 450 K given in I. Bruinsma and Zangwill [8] have given a very attractive simple model of the overlap of stress fields around boundaries and the longitudinal relaxations. This suggested that longitudinal relaxation would lead to a devil's staircase of an infinite number of stable intermediate phases, i.e. would make Δ_r negative in our case. This would clearly be very important if it were a general effect. However, we believe it cannot be so [9, 23].

6. Electronic contributions to Δ

In the last section of this paper, we estimate the intrinsic electronic contribution of ideal structures to Δ, i.e. the effect of the J_n beyond $n = 3$ in the sense of [2] and [24]. The significant values of I_1 and I_2 for SiC is surprising since I_2 already corresponds to interactions between layers distanced six bonds apart, i.e. about 7.5 Å. As discussed in previous papers [2–4, 24], particularly Shaw and Heine [24], we interpret this moderately long range as due to the remnant of what would be Friedel oscillations in a metal. The oscillations are damped in the presence of the energy gap.

Sokel and Harrison [25] have discussed this long-ranged interaction by explicitly including the band gap E_g in second-order perturbation theory. They found that the interlayer interaction energy is exponentially damped with the inverse decay length k_g where

$$k_g = [2(m_1^* + m_2^*)E_g/h^2]^{1/2}. \tag{6.1}$$

The m_1^* and m_2^* are the valence band and conduction band effective masses, taken as spherically symmetric in the model. From the limited experimental data [26], we take the average energy gap of SiC as 5 eV and the sum of effective mass as $1.0\,m_e$ where m_e is the mass of an electron. This gives a decay of interlayer interaction of one-eighteenth from the nth-neighbour double layer to the $(n+1)$th. The values of J_3 (in the notation of [2]) from previous total-energy calculations [2] is 5×10^{-4} eV per SiC pair. Thus the estimated value of J_5, which is the leading term in Δ, is about 1.6×10^{-6} eV per SiC pair. This is smaller than the phonon contribution. Another indication of the small electronic contribution to Δ is from the investigation in paper I. The calculations of the interatomic force constants in I also suggested that the analogous electronic J_n decay much more rapidly beyond J_3 than the phonon J_n, which were examined by calculating the interatomic displacement–displacement correlations. We thus expect that phonons are the dominant effect to stabilise phase $\langle 23 \rangle$ and other long-period polytypes. We also calculated the ion–ion (Ewald) contribution [2], which is part of the intrinsic electronic energy, to Δ and it turns out to be of the order of 10^{-10} eV per SiC pair. This is very small for the reasons already discussed in connection with the Ewald contribution to J_2 and J_3 [2].

We thus conclude that the electronic contributions of ideal structures to Δ is smaller than the phonon contribution. Together with the results of the relaxation calculations, we have shown that at $T = 0$ K no interactions beyond the nearest-neighbour BBI are significant enough to stabilise the phase $\langle 23 \rangle$.

References

[1] Jepps N W and Page T F 1984 *Prog. Cryst. Growth Charact.* **7** 259
Pandey D and Krishna P 1975 *J. Cryst. Growth* **31** 66; 1982 *Curr. Topics Mater. Sci.* **9** 415; 1983 *Prog. Cryst. Growth Charact.* **7** 213
[2] Cheng C, Needs R J, Heine V and Churcher N 1987 *Europhys. Lett.* **3** 475
Cheng C, Needs R J and Heine V 1988 *J. Phys. C: Solid State Phys.* **21** 1049
[3] Cheng C, Heine V and Needs R J 1990 *Phys. Rev. Lett.* submitted to *Europhys. Lett.*
[4] Cheng C, Heine V and Jones I L 1990 *J. Phys.: Condens. Matter* **2** 5097
[5] Frank F C 1987 *Phil. Mag.* A **56** 263
Pandey D and Sutton A P 1990 to be published
Pirouz P 1989 *Proc. Sixth Int. Symp. on Structure and Properties of Dislocations in Semiconductors* ed S G Roberts and P R Wilshaw (Bristol: Institute of Physics)
[6] Zhdanov G R 1945 *C.R. Acad. Sci USSR* **48** 43
[7] Safran S A and Hamann D R 1979 *Phys. Rev. Lett.* **42** 1410
[8] Bruinsma R and Zangwill A 1985 *Phys. Rev. Lett.* **55** 214
[9] Heine V 1989 *Phys. Rev. Lett.* submitted; Bruinsma R 1989 *Phase Transitions* **16/17** 275
[10] Ihm J 1982 *Rep. Prog. Phys.* **51** 105
[11] Hellmann H 1937 *Einfuhrung in die Quantenchemie* (Leipzig: Deuticke) pp 61, 285
Feynman R P 1939 *Phys. Rev.* **56** 340
[12] Nielsen O H and Martin R M 1983 *Phys. Rev. Lett.* **50** 697; 1985 *Phys. Rev.* B **32** 3780, 3792
[13] Bachelet G C, Greenside H S, Baraff G A and Schluter M 1981 *Phys. Rev.* B **24** 4745
[14] Hamann D R, Schluter M and Chiang C 1979 *Phys. Rev. Lett.* **43** 1494

[15] Churcher N, Kunc K and Heine V 1986 *J. Phys. C: Solid State Phys.* **19** 4413
[16] Monkhorst H J and Pack J D 1976 *Phys. Rev.* B **13** 5188
[17] Gomes Dacosta P, Nielsen O H and Kunc K 1986 *J. Phys. C: Solid State Phys.* **19** 3163
[18] Yean D H and Riter J R Jr 1971 *J. Phys. Chem. Solids* **32** 653
[19] Adamski R F and Merz K M 1959 *Z. Kristallogr.* **111** 350
[20] Gomes de Mesquita A H 1967 *Acta Crystallogr.* **23** 610
[21] Paxton A T, Sutton A P and Nex C M M 1987 *J. Phys. C: Solid State Phys.* **20** L263
Paxton A T 1988 *Phil. Mag.* **58** 603; 1989 *Atomistic Simulation of Materials: Beyond Pair Potentials* (New York: Plenum)
[22] Paxton A T 1989 talk in the *Total Energy Calculation Workshop (Trieste, 3–6 Jan)* (unpublished)
[23] Heine V 1990 to be published
[24] Shaw J J A and Heine V 1990 *J. Phys.: Condens. Matter* **2** 4351
[25] Sokel R and Harrison W A 1976 *Phys. Rev. Lett.* **36** 61
[26] Madelung O, Schultz M and Weiss H (ed) 1982 *Landolt-Bornstein: New Series* vol 17a *Physics of Group IV Elements and III–V Compounds* (Berlin: Springer)